Dolomitization truncates the earliest Ediacaran $\delta^{13}C_{carb}$ negative excursion

Paul Hoffman (UVic/Harvard), Galen Halverson (McGill), Marcus Kunzmann (McGill), Eric Bellefroid (Yale), Ben Johnson (UVic), Dan Schrag (Harvard). paulfhoffman@gmail.com

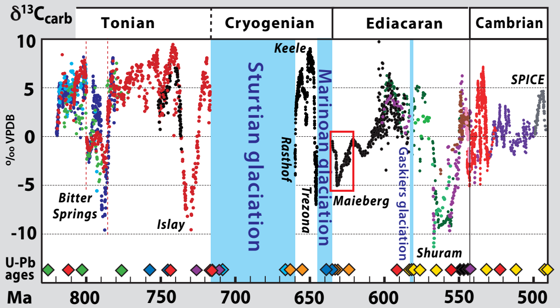

Fig. 1. Carbonate $\delta^{13}C$ record from 820 to 490 Ma (modified after Halverson et al., 2005) showing the basal Ediacaran Maieberg CIE (red box).

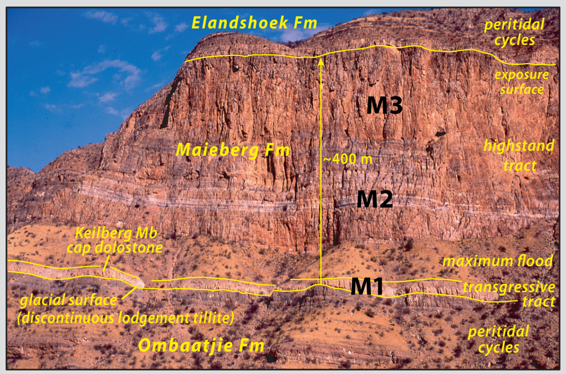

Fig. 2. Earliest Ediacaran Maieberg Formation (postglacial depositional sequence) in section 4 (see Fig. 10), upper Hoanib River near Ombaatjie, Kunene Region, Namibia.

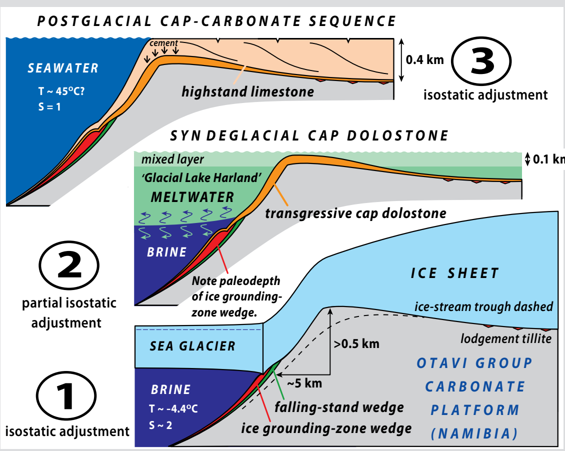

Fig. 3. Model scenario for Marinoan deglaciation and the Maieberg Fm depositional sequence. Deglaciation is assumed to generate a global meltwater lid >1.0 km deep at an average rate of 15 Sv (i.e., in 2 kyr), consuming ~6 Wm² of energy.

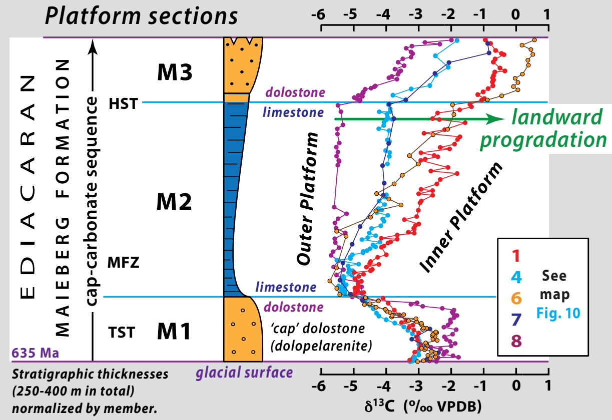

Fig. 4. Maieberg CIE in platformal sections where M2 (middle member) is limestone.

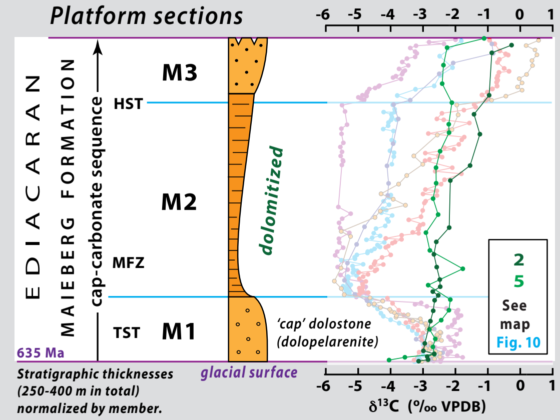

Fig. 5. Maieberg CIE in platformal sections where M2 (middle member) is dolomite. For section locations, see Fig. 10.

Abstract

The Maieberg Formation (Otavi Group) of northern Namibia offers an unusually expanded carbonate isotope record of earliest Ediacaran time (Fig. 1) and is the type example of a global negative $\delta^{13}C$ excursion, the Maieberg CIE (carbon isotope excursion). The formation presents a complete depositional sequence comprised of three members (Fig. 2): M1, a basal transgressive dolopelarenite (aka 'cap' dolostone), deposited above storm wave-base diachronously during initial syndeglacial regression and subsequent profound marine inundation; M2, a middle marly limestone rhythmite, deposited mainly below storm wave-base during maximum flooding (post-GIA); and M3, a regressive dolostone member that filled accommodation created by tectonic subsidence and erosion during the preceding Marinoan glaciation (Fig. 3). The formation is 250-400 m thick on the carbonate platform (Fig. 2), while isotopically correlative strata taper to 40 m distally on the foreslope. The negative CIE encompasses the entire formation, but its nadir at -5.5‰ PDB coincides with M2 (Fig. 4). However, where M2 is locally dolomitized, the nadir is 3‰ heavier than normal (Fig. 5), indistinguishable isotopically from M1 and M3. Moreover, the light 'tail' in the upper M1 also vanishes where M2 is dolomitized (Fig. 5), yet Mg:Ca data indicate that the light 'tail' is not correlated with calcite content. Carbonate $\delta^{18}O$ and $\delta^{13}C$ are positively correlated, both being heavier where M2 is dolomitized (Figs. 7 and 8).

Isotopic enrichments in C and CAS (carbonate associated sulfate) in areas of the platform where M2 is dolomitized were previously ascribed to restriction and lateral gradients in platform waters (Hurtgen et al., EPSL 245: 551-570, 2006). However, M2 dolomitization is also associated with CIE truncation on the unrestricted foreslope (Fig. 6), casting doubt on this explanation. Isotopic alteration during prolonged burial diagenesis (Bold et al., this session) overcomes this problem, but requires enormous volumes of solute. Whatever the mechanism, pre-existing dolomite (the M1 'tail') was evidently altered as well as limestone. Quantitatively variable expression of other CIE's may be related to alteration during burial diagenesis, particularly in areas like Namibia, where widespread chemical regmagnetization suggests long-lived groundwater flows driven by orogenic topography during the tectonic assembly of Gondwana.

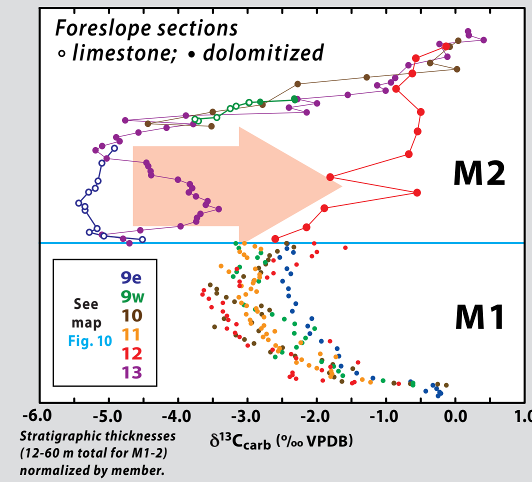

Fig. 6. Maieberg CIE in foreslope sections where M2 is marly limestone (open circles) and where it is dolomite (closed circles). Section locations, see Fig. 10.

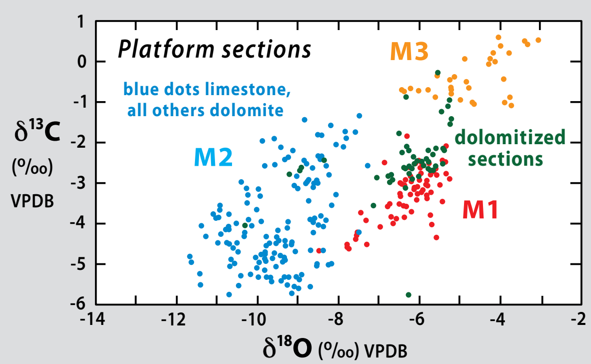

Fig. 7. Member-grouped $\delta^{13}C/\delta^{18}O$ crossplot for the platformal sections.

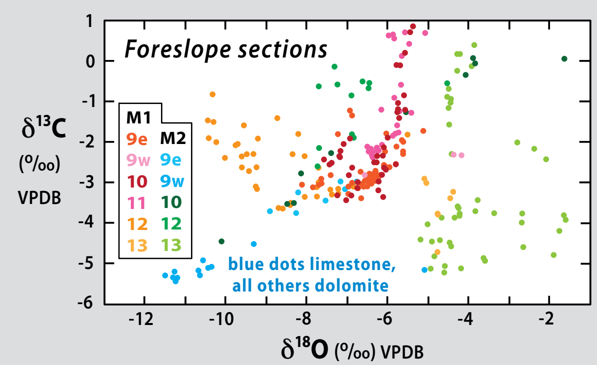

Fig. 8. Member- and site-grouped $\delta^{13}C/\delta^{18}O$ crossplot for the platformal sections.

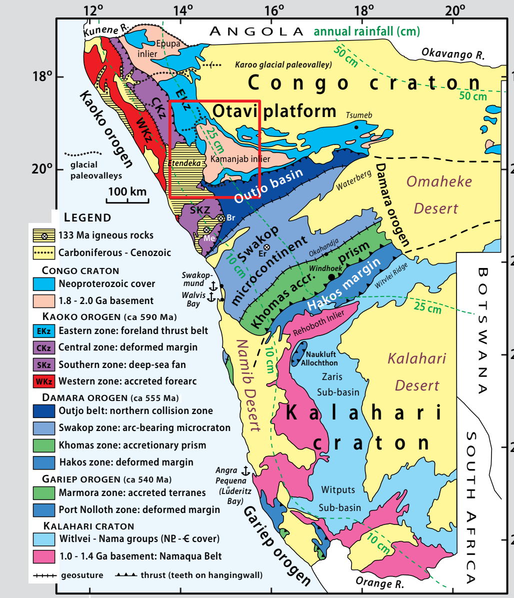

Fig. 9. Tectonic map of Namibia (SW Africa) and this study area (red box).

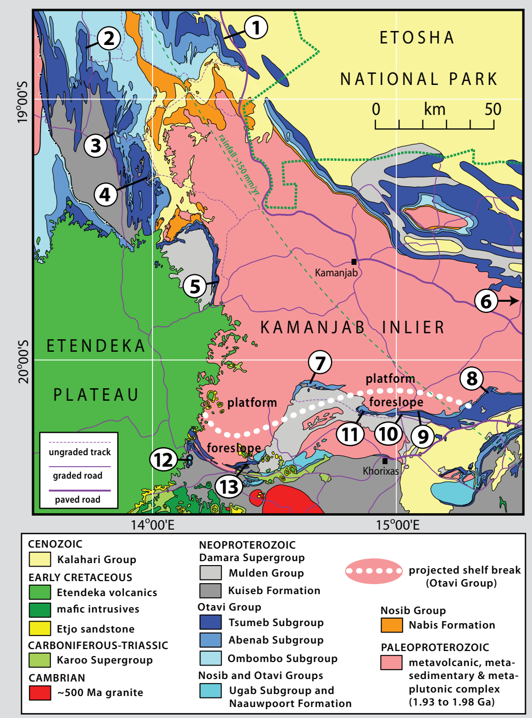

Fig. 10. Geological map with section numbers for isotope data (Figs. 4-8).